THE EFFECT OF LIPID BILAYER HYDRATION ON TRANSBILAYER PORES APPEARANCE

D. POPESCU[**], *I. STELIAN*[**], *A.G. POPESCU*[***], *NICOLETA NEACŞU*[*], *MARIA-LUISA FLONTA*[*]

[*]Department of Biophysics & Physiology, Faculty of Biology, University of Bucharest, 91–95, Splaiul Independenței, Bucharest, Romania
[**]Institute of Statistics Mathematics and Applied Mathematics, Calea 13 Septembrie, Bucharest, Romania
[***]Faculty of Automatics and Computers Control, "Politehnica" University, 313, Splaiul Independenței, Bucharest, Romania

Abstract. In this work we have determined the parameters of transbilayer pore formation induced by the collective thermal motion (CTM) of phospholipid bilayer molecules. Using the general theory of continuous elastic media we have designed a simple model of pore formation. The pore radius calculus describes in mathematical terms the lipid bilayer fluctuations, which give rise to different types of pores: open stable pores, closed stable pores (zippered pores) and unstable open pores (which determine the membrane breakdown). After bilayer deformation, the sinusoidal torus becomes an elliptical torus. Equating the volumes of these geometrical shapes, we obtain the mathematical expression of the pore radius. Comparing the pore radius with the hydrophobic bilayer thickness, the pore stability can be estimated. The effect of different degrees of polar groups hydration on the thermoporation process was analyzed.

Key word:. Hydrated lipid bilayer, pores, thermoporation and elasticity theory.

INTRODUCTION

Since their first description black lipid membranes (BLMs) were the most suitable artificial membrane models in numerous experiments which supplied important information necessary for a better understanding of the life processes occurring in living cells [50]. Beside various structures involved in membrane transport, different types of pores are also implicated (Fig. 1).

Transmembrane pores are formed in biological structures in various circumstances:

- Genetically determined pores grouped in the endothelial cells of liver sinusoid capillaries [39, 54].
- Ionophores, like the toxin gramicidin [10, 13] which following insertion in membranes, undergo a self-assembly process leading to pore formation [5, 26].

Received: August 2005;
in final form February 2006.

ROMANIAN J. BIOPHYS., Vol. 16, No.1, P. 39-56, BUCHAREST, 2006

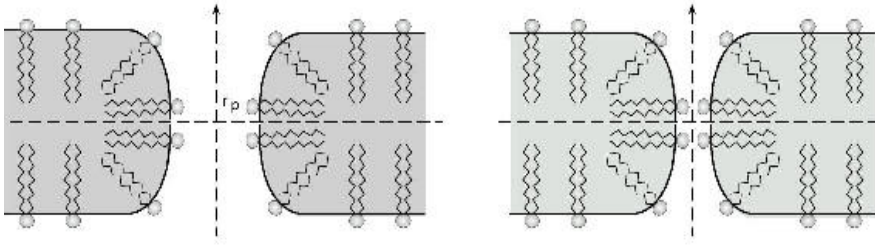

Fig. 1. Two types of pores generated by the BLM thickness fluctuations: open pores (left side), or closed pores (right side). Circles represent the polar head groups of the lipids. The pore radius is denoted by r_p.

- Stochastic lipid pores. The presence of such pores was detected in bilayers subjected to external electric fields [1]. After a period of latency from the beginning of a voltage pulse, current fluctuations (~10 pA) were noticed. These fluctuations are appearing due to superficial defects generated by polar group density fluctuations, evolving to transbilayer pores [3]. The thermal movement creates crowded regions that alternate with depopulated regions of polar groups. Within depopulated regions water comes into direct contact with hydrophobic tails and the initial superficial defect can evolve to a volume defect of the hydrophilic region. The result is that the hydrophobic pore transforms into a stable hydrophilic pore. This was the first mechanism proposed for the formation of transmembrane pores, based on lateral displacement of lipid molecules due to thermal motion [3, 32].

Theoretical biophysicists have chosen the cylindrical hydrophilic pore model [41]. In 1992, a new model of elliptical thoroidal pores was proposed [31, 32]. The model considered that pore surfaces are elliptical, covered by polar groups and the formation energy of such a stable pore equals 91 kT [32]. In addition, this model can explain the flip-flop "diffusion" of lipid molecules by diffusion along the pore surface, from one monolayer to the other [3, 23, 34]. Without explicitly specifying the way of calculating the pore energy formation, we suppose that the deformation is normal to the bilayer surface [18, 29].

Our work will provide phenomenological and theoretical proofs that local thickness fluctuations, generated by lipid molecule oscillations perpendicular to the bilayer surface, represent a novel mechanism of stochastic transbilayer pore formation. This process is called thermoporation [41, 46].

THE FREE ENERGY OF LIPID BILAYER DEFORMATION

In 1974, Pierre G. de Gennes was the first that applied the theory of elasticity of continuous media to liquid crystals [7]. Taking into account single axis smectic

liquid crystal of type A, the average orientation of the long molecular axis is described in the point *r* by the direction vector **n**(*r*) (Fig. 2).

The system of co-ordinates has its origin in the mass center of the liquid crystal with the axis *Oz* oriented perpendicularly to the surface layer.

The direction of **n**(*r*) is the same with the optical axis of the liquid crystal. In the first part of this approach, we shall consider that the elastic deformations do not induce local modifications of the liquid crystal density.

The expression of the deformation free energy, ΔF, in accord with the theory of the continuous elastic media, applied to liquid crystals, has the following form:

$$\Delta F(x,y,z) = \frac{1}{2}K_1(\text{div}\,\mathbf{n})^2 + \frac{1}{2}K_2(\mathbf{n}\times\text{curl}\,\mathbf{n})^2 + \frac{1}{2}K_3(\mathbf{n}\times\text{curl}\,\mathbf{n})^2 \quad (1)$$

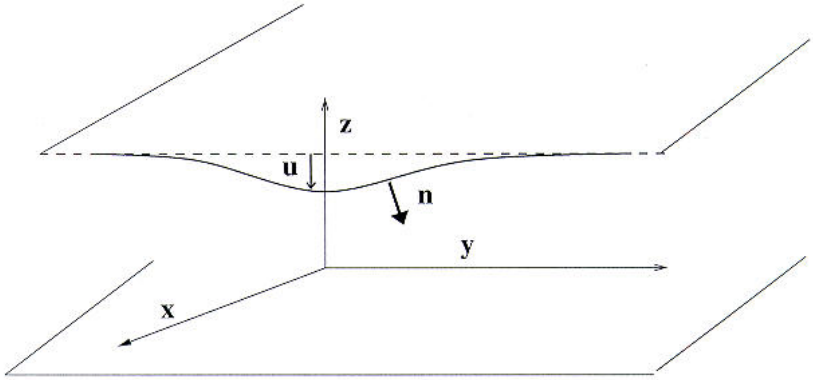

Fig. 2. The functions that describe the lipid bilayer deformation as a two layers smectic liquid crystal of type A: function *u(x,y)* that describes the deformation of the monolayer and the unity vector **n***(r)* describing the change of the initial direction of lipid molecules axis.

The crystal deformation is characterized by the direction change of the vector **n**(*r*). Its modulus is unity. However, it has a variable direction unlike a unit vector. We also assume that **n** varies slowly and smoothly with *r*. The coefficients K_i (i = 1,2,3) are positive elastic constants that correspond to each type of deformations.

The terms from equation (1) indicate the free energy of splay deformation, the torsion free energy (twist deformation) and the bending free energy, respectively. We consider the smectic liquid crystal of type A composed of many parallel and equidistant layers, so:

- The monolayer thickness is denoted by *h*.
- The component molecules, with an elongated conformation, have their long axis perpendicularly oriented to the surface layers.
- The system of co-ordinates has its origin in the mass centre of the liquid crystal with the axis *Oz* oriented perpendicularly to the surface layer.

We assume that the liquid crystal undergoes a small deformation, which is characterised by a long wavelength. The displacement of the distorted surface was denoted by *u(x,y)*, compared to its initial position (plane surface of the liquid crystal). We considerd that the molecular deviations *versus Oz* are small, and therefore neglected. In the case of an A type smectic liquid crystal, the twist and bending deformations are excluded. The new **n***(r)* components for the deformed crystal are defined by the function *u(x,y)* as it follows:

$$\begin{aligned} \mathbf{n}_x &= -\frac{\partial u}{\partial x} << 1 \\ \mathbf{n}_y &= -\frac{\partial u}{\partial y} << 1 \end{aligned} \tag{2}$$

Therefore, in this case the deformation free energy per unit area is:

$$\Delta F(x,y) = h\overline{B}\left(\frac{u}{h}\right)^2 + hK_1\left(\frac{\partial^2 u}{\partial x^2} + \frac{\partial^2 u}{\partial y^2}\right)^2 \tag{3}$$

where, $\overline{B}$ represent the elastic compression constant.

The lipid bilayer deformation is followed by the modification of its surface form and size.

The variation of the unit area, Δs, due to the BLM deformation, is given by:

$$\Delta s = \left[1 + \left(\frac{\partial u}{\partial x}\right)^2 + \left(\frac{\partial u}{\partial y}\right)^2\right]^{1/2} - 1 \cong \frac{1}{2}\left[\left(\frac{\partial u}{\partial x}\right)^2 + \left(\frac{\partial u}{\partial y}\right)^2\right] \tag{4}$$

We can obtain a complete expression for the deformation free energy per unit area if we take into account the energetic contribution caused by the change in the cross-sectional area of the BLM surface:

$$\Delta F(x,y) = h\overline{B}\left(\frac{u}{h}\right)^2 + hK_1\left(\frac{\partial^2 u}{\partial x^2} + \frac{\partial^2 u}{\partial y^2}\right)^2 + \gamma\left[\left(\frac{\partial u}{\partial x}\right)^2 + \left(\frac{\partial u}{\partial y}\right)^2\right] \tag{5}$$

where

- the first term represents the elastic compression energy of the BLM, characterised by the elastic compression constant, $\overline{B}$;
- the second term indicates the elastic energy of splay distortion, characterised by the elastic coefficient, K_1;
- the third term is the free energy due to the surface tension, characterised by the surface tension coefficient, γ.

In our case, the lipid monolayer deformation shows a cylindrical symmetry, therefore equation (5) becomes:

$$\Delta F(r) = \overline{B}\frac{u^2}{h} + hK_1\left(\frac{\partial u}{r\partial r} + \frac{\partial^2 u}{\partial r^2}\right)^2 + \gamma\left(\frac{\partial u}{\partial r}\right)^2 \tag{6}$$

The total change of the deformation free energy of BLM determined by a perturbation on a planar surface of radius *R*, is given by:

$$\Delta\overline{F} = 2\pi\int_0^R \left[\overline{B}\frac{u^2}{h} + hK_1\left(\frac{\partial u}{r\partial r} + \frac{\partial^2 u}{\partial r^2}\right)^2 + \gamma\left(\frac{\partial u}{\partial r}\right)^2\right] r dr \tag{7}$$

We have chosen as displacement function:

$$u(r,\lambda) = \pm h\cos\frac{2\pi r}{\lambda} \tag{8}$$

This is a good approximation of the exact solution of the equation which minimises the deformation energy. Unfortunately, this equation is rather complex.

The lipid zones thickness of biomembranes is not the same along the whole cell, because the lipid matrix is composed of a mixture of lipids that have hydrophobic chains of different length. These lipids selectively associate, forming different hydrophobic clusters [30]. In addition, the integral proteins produce around them a local change of the lipid bilayer [13, 41]. On the other hand, the membrane is not a static structure. The lipid bilayer surface is a dynamic succession of valleys and hills [8, 12, 14, 27]. We are interested in the perpendicular oscillations on the surface bilayer of individual lipid molecules, which are determined by thermal motion. Individual oscillations can generate a collective one, caused by interactions between lipid molecules. This local **c**ollective **t**hermal **m**otion (CTM) is the cause of the lipid bilayer thickness fluctuation. If the amplitude of the local thickness fluctuation in each monolayer, which is caused by thermal motion, is equal to the hydrophobic thickness, then the two bilayer interfaces can contact each other. Using molecular dynamic simulations we can obtain undulations and thickness fluctuations in lipid bilayers [17]. From this state the lipid bilayer can be perforated. The size of the region, occupied by lipid molecules involved in collective thermal motion (CTM), is denoted by *R*. Sometimes it is easier to use the number of lipid molecules, N_m, which is involved in collective thermal motion. Between *R* and N_m the following relation exists: $\pi R^2 = N_m a_0$ (where a_0 is the cross-sectional area of the polar head groups – see below).

Our starting hypothesis was that the bilayer deformation is caused by collective thermal motion, the single energy source for deformation. So, we can impose the condition:

$$\Delta F\left(R,\lambda\right) \le N_{\mathrm{m}}\varepsilon_{\mathrm{c}} = \frac{\pi R^2}{a_0}\left(3N - N_{\mathrm{c}}\right)\frac{k_{\mathrm{B}}T}{2} \tag{9}$$

where N_{m} is the number of phospholipid molecules involved in collective thermal motion, N is the number of atoms of a single phospholipid molecule, N_{c} the number of intra-molecular constraints (covalent bonds, angles, etc.), ε_{c} the mean kinetic energy of a phospholipid molecule, $\frac{k_{\mathrm{B}}T}{2}$ the mean kinetic energy associated to a single molecular freedom degree, h the half-thickness of the lipid bilayer and a_0 = 38.6 Å^2 [9], represents the cross-sectional area of the polar head groups. For a polyatomic molecule, we have $3N - N_{\mathrm{c}} = 6$.

Introducing function $u(r,\lambda)$ into equation (7) and performing integration over the R range, considering equal sign in (9), we obtain the equation for the wavelength λ, as a function of the size of the perturbed area.

In the next sections, we try to realize a general description of pore formation. The basic phenomenon for pore formation is the normal oscillation of lipid molecules, that induces thickness fluctuations into the lipid bilayer.

CALCULATION OF THE PORE RADIUS

A rearrangement of the molecules situated in the deformation zones may take place after perforation of the BLM. The surface of the sinusoidal torus modifies its concavity becoming the surface of a revolution elliptic torus (Fig. 3). The pore radius can be obtained equating the volumes delimited by the two revolution surfaces (i.e. sinusoidal and ellipsoidal), before the BLM perforation and after molecular rearrangement [40].

We consider the space domain, D, of an ellipsoidal torus, defined by the relations:

$$\begin{aligned} &z \in \left(0,h\right),\ r \le \lambda/4 \\ &\frac{z^2}{h^2} + \frac{\left(r-\lambda/4\right)^2}{b^2} \le 1 \end{aligned} \tag{10}$$

where b is one of the semiaxes of the ellipse, the other is equal to h.

Using a system of polar coordinates, the volume, D, of an ellipsoidal torus, is given by:

$$V = 2\pi \iint_D r \, \mathrm{d}r \, \mathrm{d}z \tag{11}$$

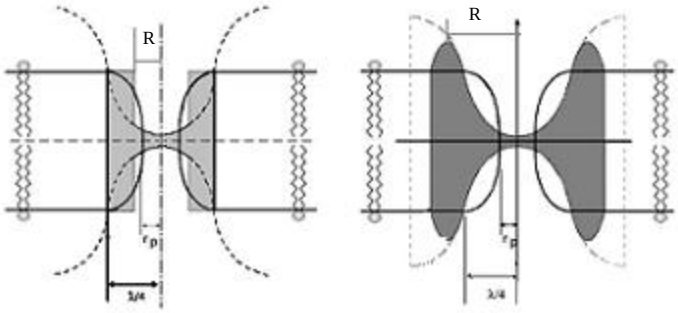

a. **b.**

Fig. 3. Cross-sectional view through the BLM deformed in the case in which the radius, *R*, of the perturbation zone is: **a.** smaller than λ/4, and **b.** greater than λ/4. λ and *r* indicate the BLM wavelength deformation and the pore radius, respectively. The lipid rearrangement starts just immediately after the BLM perforation. The molecules, which before membrane perforation belonged to the volume represented in section by the hatched region in this figure, will be refound in the volume limited by the elliptical surface of the ellipsoidal torus.

With some standard calculations, we can obtain the following expression for the volume of the **e**llipsoidal **t**orus after pore formation:

$$V_{et}(\lambda, b) = 2\pi h \begin{cases} b\left(\dfrac{\lambda\pi}{16} - \dfrac{b}{3}\right), & b \le \dfrac{\lambda}{4} \\ \dfrac{\lambda^2}{32}\sqrt{1-\left(\dfrac{\lambda}{4b}\right)^2} + \dfrac{\lambda b}{8}\arcsin\dfrac{\lambda}{4b} + \dfrac{b^2}{3}\left[\left(\sqrt{1-\left(\dfrac{\lambda}{4b}\right)^2}\right)^3 - 1\right], & b \ge \dfrac{\lambda}{4} \end{cases} \tag{12}$$

For any $R \in (\lambda/4,\ \lambda/2)$, let us define the function $f(r)$ by:

$$f(r) = \begin{cases} h\left(1 - \cos\dfrac{2\pi}{\lambda} r\right), & r \in (0, R) \\ h\left(1 - \cos\dfrac{2\pi}{\lambda}(2R - r)\right), & r \in (R, 2R - \lambda/4) \end{cases} \tag{13}$$

Using this function we define the following two domains:

$$D^{\lambda}=\left\{(z,r)\,\middle|\, r\in(0,\lambda/4),\ z\in\left(0,f(r)\right)\right\} \tag{14}$$

and

$$D_{\text{ext}}^{\lambda,R}=\left\{(z,r)\,\middle|\, r\in(\lambda/4,2R-\lambda/4),\ z\in\left(h,f(r)\right)\right\} \tag{15}$$

For $R\in(0,\lambda/4)$ we define other two domains:

$$D_{\text{int}}^{\lambda,R}=\left\{(z,r)\,\middle|\, r\in(0,R),\ z\in\left(0,f(r)\right)\right\} \tag{16}$$

and

$$G_{\text{int}}^{\lambda,R}=\left\{(z,r)\,\middle|\, r\in(R,\lambda/4),\ z\in(0,h)\right\} \tag{17}$$

Finally, we define the domain $\Omega^{\lambda,R}$ by:

$$\Omega^{\lambda,R}=\begin{cases}D^{\lambda}\cup D_{ext}^{\lambda,R}, & R\geq\lambda/4\\ G_{\text{int}}^{\lambda,R}\cup D_{\text{int}}^{\lambda,R}, & R\leq\lambda/4\end{cases} \tag{18}$$

The volume of the domain $\Omega^{\lambda,R}$, characterising a sinusoidal torus, is given by:

$$V_{st}(\lambda,R)=2\pi h\left(\frac{\lambda}{2\pi}\right)^{2}\begin{cases}\dfrac{\pi^2}{8}+1-\cos\dfrac{2\pi R}{\lambda}-\dfrac{2\pi R}{\lambda}\sin\dfrac{2\pi R}{\lambda}, & R\leq\dfrac{\lambda}{4}\\ \dfrac{\pi^2}{8}+1-\dfrac{\pi}{2}+\dfrac{4\pi R}{\lambda}\left(1-\sin\dfrac{2\pi R}{\lambda}\right), & R\geq\dfrac{\lambda}{4}\end{cases} \tag{19}$$

Equating the two volumes given by the equations (12) and (19), namely $V_{\text{et}}(\lambda,b)=V_{\text{st}}(\lambda,R)$, we can calculate the magnitude of the pore radius, *r*.

THE PROBABILITY OF TRANSBILAYER PORE APPEARANCE

According to the thermoporation mechanism analyzed in this paper, a stochastic pore may appear in a lipid bilayer, only if its deformation energy is sufficiently high for the lipid bilayer to be perforated. So, the transbilayer pore formation is a process that takes place only if an energy barrier is overcome. It happens if the probability of a pore appearance is:

$$P\propto \mathrm{e}^{-\frac{\Delta F_{\text{p}}}{k_{\text{B}}T}} \tag{20}$$

where, ΔF_p is the deformation energy for bilayer perforation, which is an increasing function of R (also of N_m).

CRITICAL RADIUS OF TRANSBILAYER PORES

Unfortunately, the continuous medium theory does not give a condition for pore stability. From this reason we will adopt a formula proposed by Lister [51] used for stochastic pores, which appear according to the mechanism of superficial defects.

According to this formula the energy of pore formation is given by:

$$\Delta F = 2\pi r\sigma - \pi r^2\gamma \tag{21}$$

where σ is the line tension (strain energy per unit length of the bilayer pore edge), and γ is the superficial tension of lipid bilayer. The critical radius and the energy barrier are:

$$r_c = \frac{\sigma}{\gamma}; \qquad \Delta F_c = \frac{\pi\sigma^2}{\gamma} \tag{22}$$

We considered that σ is equal to the superficial tension of the pore multiplied by the hydrophobic thickness, i.e. $\sigma \approx 2h\sigma_p$ [1]. Here we supposed that σ_p is approximately equal to the interfacial tension ($\sigma_p \approx \gamma/2$). In these conditions r_c is equal to the bilayer half-thickness. The exact relation between σ and σ_p is $\sigma = l_g.\sigma_p$, where l_g is the length of the rotation surface generatrice of the pore [55]. For a cylindrical pore $l_g = 2h$.

RESULTS

The hydration of the polar zone of the BLM is equivalent to the increase of the cross-section area of each polar group. In addition, a decrease of the hydrophobic thickness also happens, because the hydrophobic chains have a larger free volume [2, 15]. Most probably, the elastic compressibility coefficient, $\overline{B}$, is also modified, mainly due to the lateral compression. Figure 4 (curves 0 and 1) shows the dependence of the pore radius and of the deformation length on the perturbation region radius, when the hydrophobic thickness increases with 10Å (from 30.5 Å to 40.5 Å). This means a double number of lipid molecules that must participate in the CTM ($N \in [49–50]$ if $2h$ = 30.5 Å and $N \in [99–117]$ if $2h$ = 40.5 Å).

In order to study the hydration effect we have chosen two sets of BLMs.

The first set contains:

- the reference anhydrous BLM ($2h$ = 30.5 Å, a_0 = 38.6 Å^2, curve marked with 0);
- the hydrated BLM, which preserves its hydrophobic thickness ($2h$ = 30.5 Å, a_0 = 59 Å^2, curve marked with 1), called in the following text - hydrated BLM;
- the hydrated BLM with reduced hydrophobic thickness ($2h$ = 25.2 Å, a_0 = 59 Å^2, curve marked with 2), named hydrated and thinner BLM;

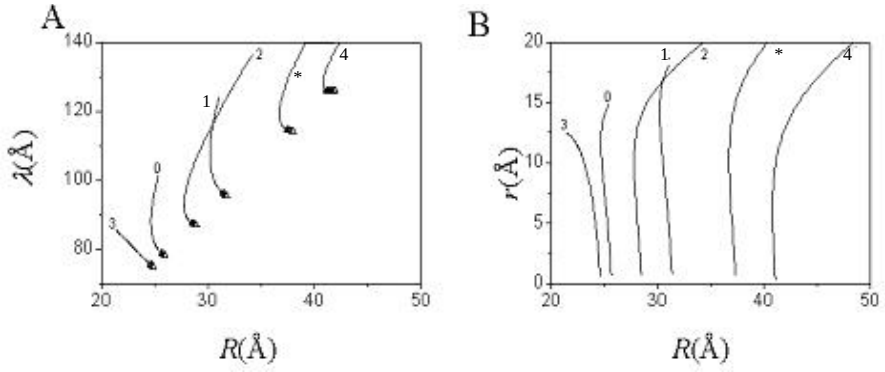

Fig. 4. Plots that illustrate the dependence of the deformation: A. wavelength of the perturbation zone radius; B. the pore radius versus the perturbation zone radius. Curves marked with zero (0) are indicated for reference BLM. Curves 1 represent planar BLM with a high cross-section area of the polar head group a_0 = 59 Å^2, $2h$ = 30.5 Å. Curves 2 represent hydrated planar BLM with $2h$ = 25.2 Å and a_0 = 59 Å^2. Curves 3 represent hydrated planar BLM with $2h$ = 25.2 Å, a_0 = 59 Å^2 B = 5×10^6 Nm^2 taking into account the change in the lateral compression. Curves marked with (*), thin non-hydrated planar BLM, with $2h$ = 40.5 Å and a_0 = 38.6 Å^2. Curves 4 represent hydrated planar BLM with $2h$ = 34 Å and a_0 = 50 Å^2. The region from each plot situated at the end of the lower branch (indicated by scattered graph) from graph (A) corresponds to closed pores. The other unspecified parameters of the lipid bilayers are identical with that of the reference BLM (curves 0). See the main text.

- the hydrated BLM for which one takes into account secondary effects: decrease of both the hydrophobic thickness and the elastic compression coefficient ($2h$ = 25.2 Å, a_0 = 59 Å^2 and B = 5×10^6 N/m^2 curve marked with 3), named soft hydrated thinner BLM.

The second set of BLMs contains only two bilayers:

- an anhydrous thicker BLM ($2h$ = 40.5 Å, a_0 = 38.6 Å^2, curve marked with *) taken as reference for the other, which is
- partially hydrated ($2h$ = 34 Å, a_0 = 59 Å^2, curve 4). The data for hydrated BLMs were taken from literature [44].

The parameters that characterize the reference lipid bilayer were determined experimentally, and have the following values:

- The hydrophobic core thickness: $2h$ = 30.5 Å [4, 54];

- The cross-section area of a lipid molecule in an anhydrous bilayer: a_0 = 38.6 Å [9];
- The splay coefficient: $K_1 = 0.933 \cdot 10^{-11}$N [6, 11, 46];
- The compressibility coefficient: $B = 5 \cdot 10^7$ N/m^2 [9]; superficial tension: $\gamma = 15 \cdot 10^{-4}$ N/m [9]. For all bilayers the temperature was T = 300 K.

The results are plotted in Fig. 4a, b.

In Tables 1 and 2 instead of the radius R, of the perturbed zone, the number of lipid molecules N_m is given, parameter that describes the size of CTM. The radii of the most probable pores for the BLMs of the first set are (see columns 2 and 3 in Table 1):

- r_{po} = 11.7 Å, for the reference BLM (its appearance conditions are: λ = 87.9Å and N_m = 49 lipid molecules);
- r_{po} = 8.1 Å, for the hydrated BLM (it appears when λ = 128 Å and N_m = 47);
- r_{po} = 9.9 Å, for the hydrated and thinner BLM (λ = 93 Å and N_m = 41);
- r_{po} = 12.5 Å, for the soft thinner hydrated BLM, (it appears when λ = 85.4 Å and N_m = 27).

Table 1

The main values of the radius (R) of the region covered by the collective thermal motion and the pores radii in the case of two unhydrated bilayers and of four hydrated ones, for which the transbilayer pore can have two states. The parameters R and r are measured in Å. N_m is the number of molecules participating simultaneously in the collective thermal motion. The closed pores are characterized by the ratio between closure distance and hydrophobic thickness (d/h). The indexes L and n were used for the pore radius in order to mark the larger pore *(L)*, or the narrow pore *(n)* as the most probable pore when there are two competitive states for a transbilayer pore.

Two pores	Open and stable		Open and stable Closed		Open and unstable Open and stable		Open and unstable Closed	
	R; (N_m)	$r_{pL;}$ r_{pn}	R; (N_m)	$r_{pL;}$ d/h(%)	R; (N_m)	$r_{pL;}$ r_{pn}	R; (N_m)	$r_{pL;}$ d/h(%)
2h=30.5 Å a_0=38.6 Å^2	24.7–25.4 (49–51)	11.7–14.8 11.7–4.0	–	– –	–	–	–	–
2h=30.5 Å a_0=59 Å^2	30.1–35.5 (47-66)	8.1–12.3 8.1–0.3	35.5–36.1 (66-68)	12.7–15.25 9.4–95				
2h=25.2Å a_0=59 Å^2	27.8–28.0 (41–42)	9.9–12.6 9.9–5.7	–	– –	28.0–28.5 (42–43)	12.6–13.9 5.7–0.7	28.5–29.0 (44–45)	13.9–14.9 9.4–94
2h=25.2Å a_0=59 Å^2 B=5·10^6 N/m^2								
2h=40.5 Å a_0=38.6 Å^2	34.6-35.2 (97-101)	11.2–16.0 11.2–0.8	35.2-35.8 (101-104)	16.0–17.4 9–93				
2h=34Å a_0=50 Å^2	36.7–37.3 (86–88)	10.2–15.0 10.23–0.6	37.3–38.0 (88–91)	15.0–16.8 9.4–94	–	–	–	–

Table 2

The main values of the radius (R) of the region covered by the collective thermal motion and of the pore radius, for the same bilayers as those from Table 1; in this case, the transbilayer pore has only one state. The parameters R and r are measured in Å. N_m is the number of molecules participating simultaneously in the collective thermal motion. The closed pores are characterized by the ratio between closure distance and hydrophobic thickness (d/h). The indexes L and n were used for pore radius, in order to mark the larger pore or the narrow pore, as the most probable pore when two competitive states for a transbilayer pore are possible.

One pore	Open and stable		Open and unstable		Closed	
	R; (N_m)	$r_{pL;}$ r_{pn}	R; (N_m)	r_{pL}	R; (N_m)	d/h(%)
$2h$=30.5 Å a_0=38.6 Å^2	25.4–25.6 (52–53)	– 4.0–0.6	–	–	25.7–26.0 (54–55)	– 9.4–94
$2h$=30.5 Å a_0=59 Å^2	–	–	36.1–53.8 (69–152)	15.25*–28.8 –	–	–
$2h$=25.2Å a_0=59 Å^2	–	–	29.0–34.2 (45–62)	14.9–19.9 –	–	–
$2h$=25.2Å a_0=59 Å^2 B=5·10^{6}N/m^2	22.5–24.2 (27–31)	– 12.5–0.6	– –	– –	24.2–24.8 (31–34)	9.4–94
$2h$=40.5 a_0=38.6 Å^2	35.8–37.9 (104–117)	17.4–20.25 –	37.9–46.7 (117–177)	20.25–27.2 –		
$2h$=34Å a_0=50 Å^2	38.0–38.7 (91–92)	16.8–17 –	38.7–123.2 (93–954)	17.0–71.1 –	–	–

DISCUSSIONS

Taking into account what we have said above, we see that for lipid bilayers with a hydrophobic thickness of 30.5 Å, the radius of the critical pore is r_c = 15.25 Å. The formation of an unstable pore in the reference BLM is impossible (Fig. 4 b, curve 0 and row 1 from Tables 1 and 2).

The compatibility range (CR) of R for hydrated BLM with big polar head groups is 30.1 Å ≤ R ≤ 53.8 Å (Fig. 1, curve 1, Tables 1 and 2, row 2). The noninjectivity range is only 30.1 Å ≤ R ≤ 36.1 Å. At these R-values only open and stable pores (8.1 Å ≤ r_p ≤ 15.25 Å) appear, for hydrated BLM with big polar head groups in competition with narrow (r_p ≤ 8.1 Å) or closed pores (Fig. 4 b, curve 1 and Table 1, row 2, columns. 3 and 5). Unstable pores will appear only if 36.1 Å ≤ R ≤ 53.8 Å, which is equivalent with a simultaneous movement of a number of lipid molecules N_m, in the range 69 ≤ N_m ≤ 152, (Table 2, row 2, col. 5).

In the case of hydrated and thinner BLMs (Fig. 4 b, curve 2, row 3 from Tables 1 and 2) the radius of the critical pore is equal to r_c = 12.6 Å, owing to the decrease of the hydrophobic thickness which follows the hydration of the polar region. These values correspond to *R*-values from the noninjectivity part of CR, so an additional combination of pore states will appear compared to the corresponding anhydrous BLMs. For example:

- If 41–42 molecules generate the perturbation of BLMs surface, both pores may be open and stable. The larger pore has its radius 9.9 Å ≤ r_p ≤ 12.6 Å and the narrow pore has its radius 5.7 Å ≤ r_p ≤ 9.9 Å and (Table 1, row 3, col. 3).
- If simultaneous and normal movements of 42–45 molecules generate the perturbation of the bilayer surface, then the larger pore is unstable because it has its radius greater than the critical one (r_c= 12.6 ≤ r_p ≤ 14.9 Å) and the narrow pore has its radius r_p ≤ 5.7 Å or it is closed (Table 1, row 3, col. 7 and 9).
- If 45–62 molecules are involved in the CTM, the pore has only an unstable state (r_c < 14.9 Å ≤ r_p ≤ 19 Å), the open pore is unstable (Table 2, row 3, col. 5).
- There is only a single pore open and stable (r_p ≤ 12.5 Å) or a closed one for the modified BLM due to all secondary effects of hydration, becoming thinner and soft (Table 2, row 4, col. 3 and 7, respectively).

A hydrated BLM obtained from a lipid BLM with a big hydrophobic core thickness is more resistant to thermoporation. This may be seen in Fig. 4 a, b on the curves marked with * and 4 (and in Tables 1 and 2, rows 5 and 6), corresponding to the lipid BLMs of the second set. For the anhydrous BLM, r_c = 20.25 Å, while for hydrated one r_c = 17 Å. The pairs of pores states remain available for both BLMs. So, for the anhydrous BLM the uninjectivity part of CR is 34.6 Å ≤ *R* ≤ 35.8 Å (97 ≤ N_m ≤ 104) (Table 1, row 5, cols. 2 and 4). For each of these values of *R* the appearance of a larger and stable pore (11.2 Å ≤ r_p ≤ 17.4 Å) is possible, as an alternative to a narrow pore (r_p ≤ 11.2 Å) or a closed one (Table 1, row 5, cols. 3 and 5).

For *R*-values from the bijection range an open pore which is stable may appear (17.4 Å ≤ r_p ≤ 20.25 Å) if 35.8 Å ≤ *R* ≤ 37.9 Å (Fig. 4 b, curve marked with *, Table 2, row 5, col. 3), or an open and unstable pore (20.25 Å ≤ r_p ≤ 27.2 Å) can appear, if 37.9 ≤ *R* ≤ 46.7 Å (117 ≤ N_m ≤ 177) (Fig. 4 b, curve marked with *, Table 2, row 5, col. 5).

For the corresponding hydrated BLM the things are similar**.** For the noninjectivity range, 36.7 Å ≤ *R* ≤ 38 Å, (86 ≤ N_m ≤ 91) pairs of stable pores may appear: one is larger 10.2 Å ≤ r_p ≤ 16.8 and the other is narrow, r_p ≤ 10.2 Å or closed (Fig. 4 b, curve 4, Table 1, row 6, cols. 3 and 5).

A single open and stable pore may be generated if 38 Å ≤ *R* ≤ 38.7 Å (91 ≤ N_m ≤ 92) with a radius 16.8 Å ≤ r_p ≤ 17 Å = r_c (Fig. 4 b, curve 4, Table 2, row 6, col. 3). For the last part of CR 38.7 Å ≤ *R* ≤123.2 Å (91 ≤ N_m ≤ 954) an unstable pore (17Å ≤ r_p ≤ 71Å) may appear (Fig. 4 b, curve 4, Table 2, row 6, col. 5).

As we can see in Table 1, in the generation of pores by collective thermal motion a small number of molecules are involved, so we believe that the pores appearance caused by the thickness fluctuations is quite plausible. Recently these pores were obtained by molecular dynamics simulation [56]. In many cases approached in this text, values of collective thermal motion magnitude expressed by *R*-values, for which pores can have two states, can be found.

From the energetical point of view, these two states, corresponding to the same value of *R*, are equally probable, because ΔF_p from eq. (20) does not change. As we have already mentioned, the value of the deformation wavelength determines in which state the pore may appear. In some cases the translation of a pore from a state to another is determined by a small change in the *R*-value (about fractions of Å) or in the number of lipid molecules from CTM (one or two molecules) as given in Table 1, rows 3, for example. In these situations we can see the importance of the wavelength in bilayer deformation, which is determined by the initial dephasing existent between the molecules participating in the collective thermal motion.

On the other hand, an interchange of lipid molecules (those from the bottom of the deformation) between the two monolayers is possible without the bilayer perforation. In other words, the flip-flop phenomenon is possible without pore generation. The molecules located in the central deformation region of the two monolayers, which can have the polar groups in the median plane of the BLM, can realize a very stable configuration by antiparallel coupling of their electrical dipoles. If the BLM will not generate the formation of a pore, but evoluates towards elimination of the deformation, the two coupled molecules (one from each monolayer) will remain in one of the two monolayers. In addition, the flip-flop phenomenon can also take place by diffusion of the molecules on the formed pore surface, which in certain conditions can disappear.

The probability of stable pore appearance increases following hydration. This is because the number of lipid molecules necessary for stable pore formation decreases after hydration of lipid BLM. On the other hand, for the thinner hydrated BLMs, the thermoporation is less probable.

The decrease of the elastic constant of compression, especially due to the lateral compression, must be also considered. These observations are relevant for liposomes, which are used as drug carriers. We have to add that in the text the value of lipid molecule number is referring only to the molecules from a monolayer.

CONCLUSIONS

The thickness of a lipid bilayer, formed from a lipid mixture, is not constant along the entire bilayer, for two reasons:

- bilayer phospholipids have hydrophobic chains of different lengths;
- selective associations happen between molecules [21, 22, 23, 30, 35].

The result of these selective associations in BLMs consists in the formation of clusters separated by microinterfaces [13, 14, 15, 20, 31].

These clusters form different thickness regions, depending on the lengths of the molecular chains that have contributed to their occurrence [24, 36, 37, 38]. These thickness variations overlap with lipid molecule fluctuations perpendicular to the surface due to thermal motion. It is possible that a monolayer deformation overlap with another monolayer deformation. The amplitudes of both deformations can be equal to the half thickness of the bilayer. In this situation, the lipid bilayer breakdown can produce pores generated by thickness fluctuations and determined by thermal movements of lipid molecules perpendicular to the surface. Generally, lipid bilayers, either artificial or natural, are not homogeneous.

The pore formation mechanism by thermal fluctuations is not yet well understood, still being a matter of challenge and controversies. We tried to demonstrate that the general theory of continuous elastic media could predict the generation of all types of pores generated by the BLM thermal fluctuations of thickness. The thermal energy necessary to cause BLM deformation is proportional to R^2. Therefore, the closer to R_m is the radius of the collective thermal motion zone, the greater the probability is for a pore to appear.

The closed pores resulting from the coupling between the polar head group dipoles can be very stable. The space between the polar head groups is filled with a row of water molecules. Practically, the closed pore radius is not zero.

Our results, obtained by application of the general theory of continuous elastic media to the BLM elasticity**,** confirm the existence of a new mechanism of transbilayer pore formation. The mechanism of pore formation is based on the variation of BLM thickness due to the collective thermal motion, but it does not exclude the surface defects induced by lateral thermal motions.

REFERENCES

1. ABIDOR, I.G., V.B. ARAKELIAN, L.V. CHERNOMORDIK, Yu.A. CHIZMADZHEV, V.F. PASTUSHENKO, M.R. TARASEVICH, Electric breakdown of bilayer lipid membranes. I. The main experimental facts and their qualitative discussion, *Bioelectrochem. Bioenerg.*, 1979, **6**, 37–52.
2. BULDT, G., H.U. GALLY, A. SEELING, J. SEELING, G. ZACCAI, Neutron diffraction studies on selectively deuterated phospholipid bilayers, *Nature (London)*, 1978, **271**, 182–184.
3. CHIZMADZHEV, YU.A., V.B. ARAKELIAN, V.F. PASTUSHENKO, Electric breakdown of bilayer lipid membranes. III. Analysis of possible mechanism of defect origination, *Bioelectrochem. Bioenerg.*, 1979, **6**, 63–70.
4. DILGER, J.P., The thickness of monoolein lipid bilayers as determined from reflectance measurements, *Biochim. Biophys. Acta*, 1981, **645**, 357–363.
5. ELLIOT, J.R., D. NEEDHAM, J.P. DILGER, D.A. HAYDON, The effects of bilayer thickness and tension on gramicidin single-channel lifetime, *Biochim. Biophys. Acta*, 1983, **735**, 95–103.

6. ENGELHARDT, H., H.P. DUWE, E. SACKMAN, Bilayer bending elasticity measurement by Fourier analysis of thermally excited surface undulations of flaccid vesicles, *J. Physique Lett.*, 1985, **46**, L-395-L-400.
7. DE GENNES, P.G., *The Physics of Liquid Crystals*, Clarendon Press, Oxford, 1974.
8. GRUEN, D.W.R., S. MARCELJA, V.A. PARSEGIAN, *Cell Surface Dynamics*, Dekker, New York, 1984.
9. HLADKY, S.B., D.W.R. GRUEN, Thickness fluctuations in black lipid membranes, *Biophys. J.*, 1982, **38**, 251–258.
10. HELFRICH, P., E. JAKOBSSON, Calculation of deformation energies and conformations in lipid membranes containing gramicidin channels, *Biophys. J.*, 1990, **57**, 1075–1084.
11. HELFRICH, W., Elastic properties of lipid bilayers: theory and possible experiments, *Z. Naturforsch.*, 1973, **28C**, 693–703.
12. HONING, B., K. SHARP, A.S. YANG, Microscopic models of aqueous solutions: biological and chemical applications, *J. Phys. Chem*., 1993, **97**,1101–1109.
13. HUANG, H.W., Deformation free energy of bilayer membrane and its effect on gramicidin channel lifetime, *Biophys. J.*, 1986, **50**, 1061–1070.
14. ISRAELACHVILI, J.N., S. MARCELJA, R.G. HORN, Physical principles of membrane organization, *Quarterly Rev. Biophys.*, 1980, **13(2)**, 121–200.
15. JAIN, M.K., *Membrane Fluidity in Biology*, Academic Press, London, 1983.
16. JORGENSEN, K., M.M. SPEROTTO, O.G. MOURITSEN, J.H. IPSEN, M.J. ZUCKERMANN, Phase equilibria and local structure in binary lipid bilayers, *Biochim. Biophys. Acta*, 1993, **1152**, 135–145.
17. LINDAHL, E., O. EDHOLM, Mesoscopic Undulations and Thickness Fluctuations in Lipid Bilayers from Molecular Dynamics Simulations, *Biophys. J.*, 2000, **79**, 426–433.
18. MILLER, I.R., Energetics of fluctuations in lipid bilayer thickness, *Biophys. J.*, 1984, **45**, 643–644.
19. MOURITSEN, O.G., M. BLOOM, Models of lipid-protein interactions in membranes, *Annu. Rev. Biophys. Biomol. Struct*., 1993, **22**, 147–171.
20. MOVILEANU, L., H. BAYLEY, Stability of lipid bilayers and red blood cell membranes, *Phys. Lett*., 2001, **A53** (1975) 193–194.
21. MOVILEANU, L., D. POPESCU, Aspects of self- and cross-association hydrophobicity into single chain binary mixtures. A computer study, *Acta Biochimica Polonica*, 1995, **42(1)**, 89–96.
22. MOVILEANU, L., D. POPESCU, Differential effects on the association probabilities: A 3-D approach, *Biosystems*, 1995, **36**, 43–53.
23. MOVILEANU, L., D. POPESCU, G. VICTOR, G. TURCU, Selective association of phospholipids as a clue for the passive flip-flop diffusion through bilayer lipid membranes, *Biosystems*, 1997, **40**, 263–275.
24. MOVILEANU, L., D. POPESCU, MARIA-LUIZA FLONTA, The hydrophobic acyl chain effect in the lipid domains appearance through phospholipid bilayers, *Journal of Molecular Structure (THEOCHEM)*, 1998, **434**, 213–227.
25. MOVILEANU, L., D. POPESCU, A theoretical model for the association probabilities of saturated phospholipids from two component biological lipid membranes, *Acta Biotheor.*, 1999, **46**, 347–368.
26. MOVILEANU, L., H. BAYLEY, Partitioning of a polymer into a nanoscopic protein pore obeys a simple scaling law, *Proc. Natl. Acad. Sci. USA*, 2001, **98**, 10137–1014.
27. MOVILEANU, L., D. POPESCU, S. ION, A. POPESCU**,** Transbilayer pores induced by thickness fluctuations**,** *Bul. Math Biol*., 2005, in press.
28. MOWALD, H., Surfactant layers at water surfaces, *Rep. Prog. Phys*. 1993, **56**, 653–685.
29. PETRACHE, H.I., S. TRISTRAM-NAGLE, J.F. NAGLE, Fluid phase structure of EPC and DMPC bilayers, *Chem. Phys. Lipids*, 1998, **95**, 83–94.
30. POPESCU, D., D.-G. MĂRGINEANU, Intramembrane interactions and breakdown of lipid bilayers, *Bioelectrochem. Bioenerg*. 1981, **8**, 581–583.
31. POPESCU, D., G. VICTOR, Association probabilities between the single chain amphiphiles into binary mixtures, *Biochim. Biophys. Acta*, 1990, **1030**, 238–250.

32. POPESCU, D., The calculation of the optimal surface for amphiphile molecules using the hard core method, *Biophys. Chem.*, 1991, **39**, 283–286.
33. POPESCU, D., C. RUCĂREANU, G. VICTOR, A model for the appearance of the statistical pores in membranes due to the selfoscillations, *Bioelectrochem. Bioenerg*., 1991, **25**, 91–105
34. POPESCU, D., The transversal diffusion coefficient of phospholipid molecules through black lipid membranes, *Bioelectrochem. Bioenerg.*, 1991, **25**, 105–108.
35. POPESCU, D., C. RUCĂREANU, Membrane selfoscillations model for the transbilayer statistical pores and flip-flop diffusion, *Mol. Cryst. Liq. Cryst.*, 1992, **215**, 339–348
36. POPESCU, D., Association probabilities between single chain amphiphiles into a binary mixture in plane monolayers (II), *Biochim. Biophys. Acta*, 1993, **1152**, 35–43.
37. POPESCU, D., Selective association processes of mixed phospholipids in monolayer films, *Biophys. Chem.*, 1994, **48**, 369–381.
38. POPESCU, D., L. MOVILEANU, Global ratio of efficiency in a single chain binary mixture, *J. Biol. Syst.*, 1996, **4(3)**, 425–432.
39. POPESCU, D., L. MOVILEANU, G. VICTOR, G. TURCU, Stability and instability properties of aggregation of single chain amphiphiles into binary mixtures, *Bulletin of Mathematical Biology*, 1997, **50(1)**, 60–78.
40. POPESCU, D., L. MOVILEANU, S. ION, MARIA LUIZA FLONTA, Hydrodynamic effects on the solute transport across endothelial pores and hepatocyte membranes, *Phys. Med. Biol.*, 2000, **45**, N157-N165.
41. POPESCU, D., L. MOVILEANU, S. ION, FLORENTINA PLUTEANU, SPERANTA AVRAM, D. MARINESCU, MARIA LUIZA FLONTA, The elastic waves induce the appearance of pores in a lipid bilayer membrane (II), *Romanian J. Biophys*, 2001, **11 (3-4)**, 163–170.
42. POPESCU, D., S. ION, A. POPESCU, L. MOVILEANU, Elastic properties of BLMs and pore formation, *In: Black Lipid Membranes (BLMs) and Their Applications*, Elsevier, Amsterdam, 2002.
43. RAREY M., B. Kramer, and T. Lengauer. The particle concept: Placing discrete water molecules during protein-ligand docking predictions. *Proteins*, 1999, **34(1)**, 17–28.
44. RAWICZ, W., K.C. OLBRICH, T. MCINTOSH, D. NEEDHAM, E. EVANS, Effect of chain length and unsaturation on elasticity of lipid bilayers, *Biophys. J.*, 2000, **79**, 328–339.
45. SCHNEIDER, M.B., J.T. JENKINS, W.W. WEBB, Thermal fluctuations of large quasi-spherical bimolecular phospholipid vesicles, *J. Physique*, 1984, **45**, 1457–1472.
46. SHARP, K.A., B. HONING, Electrostatic interactions in macromolecules: Theory and applications, *Annu. Rev. Biophys. Biophys. Chem*., 1990, **19**, 301–332.
47. SHILLCOCK, J.C., U. SEIFERT, Thermally induced proliferation of pores in a model fluid membrane, *Biophys. J*., 1998, **74**, 1754–1766.
48. SILVER, B.L., *The Physical Chemistry of Membranes*, Allen & Unwin, London, 1985.
49. STEPHEN, M.J., J.P. STRALEY, Physics of liquid crystals, *Rev. Mod. Phys*., 1974, **46**, 617–704.
50. TANFORD, C., The Hydrophobic Effect: Formation of Micelles and Biological Membranes, 2nd edition, John Wiley, New York, 2000.
51. TIELMAN, D.P., H. LEONTIADOU, A.E. MARK, S.J. MARRINK, Simulation of pore formation in lipid bilayers by mechanical stress and electric fields, *J. Amer. Chem. Soc*., 2003, **125,** 6382–6383.
52. TIEN, H.T., A. OTTOVA-LEITMANNOVA, *Membrane Biophysics as Viewed from Experimental Bilayer Lipid Membranes*, Elsevier, Amsterdam and New York, 2000.
53. WEAVER, J.C., R.A. MINTZER, Decreased bilayer stability due to transmembrane potentials, *Phys. Lett.*, 1981, **86A(1)**, 57–59.
54. WEAVER, J.C., YU.A. CHIZMADZHEV, Theory of electroporation: A review, Bioelectrochem, *Bioenerg.*, 1996, **41**, 135–160.
55. WHITE, S.H., Formation of solvent-free black lipid bilayer membranes from glyceryl monooleate dispersed in squalene, *Biophys. J*., 1978, **23**, 337–347.
56. WISSE, E., An electron microscopic study of the fenestrated endothelial lining of rat liver sinusoids, *J. Ultrastruct. Res*., 1970, **31**, 125–150.